FINNISH METEOROLOGICAL INSTITUTE
CONTRIBUTIONS

NO. 76

TOWARDS THE USE OF RADAR WINDS IN NUMERICAL WEATHER PREDICTION

Kirsti Salonen

Department of Physics
Faculty of Science
University of Helsinki
Helsinki, Finland

ACADEMIC DISSERTATION in meteorology

To be presented, with the permission of the Faculty of Science of the University of Helsinki, for public criticism in Auditorium Chemicum A129 (A.I. Virtasen Aukio 1) on January 30th, 2009, at 12 o'clock noon.

Finnish Meteorological Institute
Helsinki, 2008

ISBN 978-951-697-683-2 (paperback)
ISSN 0782-6117
Yliopistopaino
Helsinki, 2008

ISBN 978-951-697-684-9 (PDF)
http://ethesis.helsinki.fi
Helsinki, 2008

FINNISH METEOROLOGICAL INSTITUTE

Published by Finnish Meteorological Institute

P.O. Box 503
FIN-00101 Helsinki, Finland

Series title, number and report code of publication
Finnish Meteorological Institute
Contributions 76, FMI-CONT-76

Date
December 2008

Author
Kirsti Salonen

Name of project

Commissioned by

Title
Towards the use of radar winds in numerical weather prediction

Abstract
Numerical weather prediction (NWP) models provide the basis for weather forecasting by simulating the evolution of the atmospheric state. A good forecast requires that the initial state of the atmosphere is known accurately, and that the NWP model is a realistic representation of the atmosphere. Data assimilation methods are used to produce initial conditions for NWP models. The NWP model background field, typically a short-range forecast, is updated with observations in a statistically optimal way. The objective in this thesis has been to develope methods in order to allow data assimilation of Doppler radar radial wind observations. The work has been carried out in the High Resolution Limited Area Model (HIRLAM) 3-dimensional variational data assimilation framework.

Observation modelling is a key element in exploiting indirect observations of the model variables. In the radar radial wind observation modelling, the vertical model wind profile is interpolated to the observation location, and the projection of the model wind vector on the radar pulse path is calculated. The vertical broadening of the radar pulse volume, and the bending of the radar pulse path due to atmospheric conditions are taken into account. Radar radial wind observations are modelled within observation errors which consist of instrumental, modelling, and representativeness errors. Systematic and random modelling errors can be minimized by accurate observation modelling. The impact of the random part of the instrumental and representativeness errors can be decreased by calculating spatial averages from the raw observations. Model experiments indicate that the spatial averaging clearly improves the fit of the radial wind observations to the model in terms of observation minus model background (OmB) standard deviation.

Monitoring the quality of the observations is an important aspect, especially when a new observation type is introduced into a data assimilation system. Calculating the bias for radial wind observations in a conventional way can result in zero even in case there are systematic differences in the wind speed and/or direction. A bias estimation method designed for this observation type is introduced in the thesis. Doppler radar radial wind observation modelling, together with the bias estimation method, enables the exploitation of the radial wind observations also for NWP model validation. The one-month model experiments performed with the HIRLAM model versions differing only in a surface stress parameterization detail indicate that the use of radar wind observations in NWP model validation is very beneficial.

Publishing unit
Finnish Meteorological Institute, Meteorological Research Unit

Classification (UDC)
551.509.313.22
551.509.313.42
551.508.855

Keywords
wind observation, data assimilation, remote sensing, weather radar, numerical weather prediction

ISSN and series title
0782-6117 Finnish Meteorological Institute Contributions

ISBN
978-951-697-683-2 (paperback), 978-951-697-684-9 (pdf)

Language
English

Pages
87

Price

Sold by
Finnish Meteorological Institute / Library
P.O. Box 503, FIN-00101 Helsinki, Finland

Note

ILMATIETEEN LAITOS

Julkaisija Ilmatieteen laitos

PL 503, 00101 Helsinki

Julkaisun sarja, numero ja raporttikoodi
Finnish Meteorological Institute
Contributions 76, FMI-CONT-76

Julkaisuaika
Joulukuu 2008

Tekijä
Kirsti Salonen

Projektin nimi

Toimeksiantaja

Nimike
Kohti tutkatuulihavaintojen hyödyntämistä numeerisissa sääennustusmalleissa

Tiivistelmä

Sääennustusmallilla simuloidaan ilmakehän tilan kehitystä ratkaisemalla ilmakehää kuvaava yhtälöryhmä numeerisesti. Ennusteen onnistumisen kannalta on tärkeää, että mallin alkutila kuvaa mahdollisimman hyvin ilmakehän todellista tilaa ennusteen alkuhetkellä ja että malli itsessään kuvaa ilmakehän käyttäytymistä mahdollisimman realistisesti. Mallin alkutilan määrittämisessä käytetään data-assimilaatiomenetelmiä, jotka yhdistävät havaintotiedon ja mallitiedon tilastollisesti optimaalisella tavalla. Tämän väitöskirjatyön tavoite on ollut kehittää menetelmiä säätutkalla mitattujen säteen suuntaisten tuulihavaintojen (jatkossa tutkatuulihavainto) hyödyntämiseksi numeerisissa sääennustusmalleissa. Työssä on käytetty High Resolution Limited Area Model (HIRLAM) rajoitetun alueen sääennustusmallia.

Havainnon tarkka mallintaminen on tärkeää, kun hyödynnetään sellaisia havaintotyyppejä, jotka eivät ole sääennustusmallin muuttujia. Tutkatuulihavainto mallinnetaan interpoloimalla sääennustusmallin tuuliprofiili havaintopisteeseen ja laskemalla mallin tuulivektorin projektio tutkasäteen suunnassa. Havainnon mallinnuksessa huomioidaan tutkakeilan leveneminen mittausetäisyyden kasvaessa ja ilmakehän olosuhteista riippuva tutkasäteen taipuminen. Tutkatuulihavainto mallinnetaan havaintovirheiden puitteissa. Havaintovirheet koostuvat instrumentti-, mallinnus- ja edustavuusvirheistä. Havainnon tarkalla mallintamisella voidaan minimoida systemaattisia ja satunnaisia mallinnusvirheitä. Satunnaisia instrumentti- ja edustavuusvirheitä voidaan vähentää laskemalla tutkahavainnoista aluekeskiarvoja, nk. superhavaintoja.

Havaintojen laadunvalvonta on tärkeää etenkin silloin, kun mallin analyysijärjestelmässä otetaan käyttöön uusi havaintotyyppi. Tutkasäteen suuntaisten tuulihavaintojen kohdalla perinteisesti laskettu harha on usein lähellä nollaa, vaikka havainnoissa olisikin systemaattisia virheitä. Tässä väitöskirjatyössä on kehitetty tutkatuulihavainnoille harhan estimointimenetelmä, jossa otetaan huomioon tutkatuulimittauksen tyypilliset ominaisuudet. Tutkatuulihavainnon tarkka mallintaminen ja harhan estimointimenetelmä mahdollistavat havaintotyypin käyttämisen myös sääennustusmallien validoinnissa. Vertaamalla kahta HIRLAM mallin versiota, joissa pintastressin parametrisointi on toteutettu hieman toisistaan poikkeavalla tavalla, on osoitettu, että tutkatuulihavaintojen käyttäminen sääennustusmallin validoinnissa on erittäin hyödyllistä.

Julkaisijayksikkö
Meteorologinen tutkimus

Luokitus (UDK)
551.509.313.22
551.509.313.42
551.508.855

Asiasanat
tuulihavainto, data-assimilaatio, säätutka, kaukokartoitus, numeerinen sääennustusmalli

ISSN ja avainnimike
0782-6117 Finnish Meteorological Institute Contributions

ISBN
978-951-697-683-2 (paperback), 978-951-697-684-9 (pdf)

Kieli
englanti

Sivumäärä
87

Hinta

Myynti
Ilmatieteen laitos / Kirjasto
PL 503, 00101 Helsinki

Lisätietoja

Drawing by Kirsti, 3rd March 1984
at Raimo Pulkkinen’s dissertation.

PREFACE

The work presented in this thesis has been carried out at the Meteorological Research unit of the Finnish Meteorological Institute (FMI) in 2002–2008 and has been financially supported by the Academy of Finland.

I would like to express my gratitude to my supervisor, Prof. Heikki Järvinen, for guiding me from my young undergraduate student days to this stage. I thank him especially for providing innovative ideas, critical views, and support for my work during all these years. I also wish to thank Prof. Hannu Savijärvi at the University of Helsinki for his encouragement and support.

My gratitude is due to Prof. Mikko Alestalo for employing me in the numerical weather prediction group of FMI. I would also like to thank the former Section head, Dr. Juhani Damski, as well as the current head Prof. Sylvain Joffre, for providing support and the opportunity to complete this work. I thank all of my colleagues in the numerical weather prediction group, in particular its leader Dr. Carl Fortelius, for useful discussions and for creating a warm and friendly working environment.

I thank Prof. Heikki Haario, Lappeenranta University of Technology, and Dr. Stéphane Laroche, Environment Canada, for reviewing this thesis and for their suggestions towards improving the manuscript.

I wish to thank my co-authors Reima Eresmaa, Günther Haase, Asko Huuskonen, Magnus Lindskog, Sami Niemelä, and Simo Järvenoja, (who is sadly no longer with us), for their fruitful co-operation and discussions. I would also like to thank the FMI radar team for deepening my radar knowledge and for organizing many enjoyable occasions.

I express my gratitude to my parents, Vappu and Lasse, and my sister Tarja and her family for constant support. I would like to thank my dear friends for being sympathetic listeners, and also for taking care that I remember that there is also life outside work. Finally, I wish to thank Heikki for encouraging me to face the challenges arising, and for bringing special happiness into my life.

Helsinki, November 2008

Kirsti Salonen

Contents

LIST OF ORIGINAL PUBLICATIONS

I Järvinen, H, Salonen, K, Lindskog, M, Huuskonen, A, Niemelä, S and R Eresmaa, 2008: Doppler radar radial winds in HIRLAM. Part I: Observation modelling and validation. *Tellus* **A**, accepted for publication.

II Salonen, K, Järvinen, H, Haase, G, Niemelä, S and R Eresmaa, 2008: Doppler radar radial winds in HIRLAM. Part II: Optimizing the super-observation processing. *Tellus* **A**, accepted for publication.

III Salonen, K, Järvinen, H, Eresmaa, R and S Niemelä, 2007: Bias estimation of Doppler-radar radial-wind observations. *Quarterly Journal of the Royal Meteorological Society*, **133**: 1501–1507.

IV Salonen, K, Järvinen, H, Järvenoja, S, Niemelä, S and R Eresmaa, 2008: Doppler Radar Radial Wind Data in NWP model validation. *Meteorological Applications*, **15**: 97–102.

SUMMARIES OF THE ORIGINAL PUBLICATIONS

The contents of PAPERS I–IV and the author's contribution are briefly outlined below.

I Järvinen, H, Salonen, K, Lindskog, M, Huuskonen, A, Niemelä, S and R Eresmaa, 2008: Doppler radar radial winds in HIRLAM. Part I: Observation modelling and validation. *Tellus* **A**, accepted for publication.

PAPER I describes the Doppler radar radial wind measurement and its modelling in detail. The observation operator developed has been incorporated into the HIRLAM limited area numerical weather prediction (NWP) system, and has been tested in a one-month model experiment in which the radar radial wind data were passively monitored against the model counterparts. The author of this thesis has contributed to the observation operator design and is responsible for coding the radar pulse volume broadening and the pulse path bending due to refraction. The author is also responsible for all the experimentation and for a significant part of the writing.

II Salonen, K, Järvinen, H, Haase, G, Niemelä, S and R Eresmaa, 2008: Doppler radar radial winds in HIRLAM. Part II: Optimizing the super-observation processing. *Tellus* **A**, accepted for publication.

PAPER II considers the optimal Doppler radar radial wind processing strategy for varying NWP model resolutions. The radar radial wind observations are modelled within observation errors arising from instrumental, modelling and representativeness sources. The impact of the random part of the instrumental and representativeness errors can be decreased by calculating spatial averages, so-called super-observations, from the raw observations. The HIRLAM model experiments indicate that the generation of super-observations does not improve the fit of the radial wind observations to the model in terms of bias. However, the impact of random observation errors is reduced. The author is responsible for all the experimentation and for most of the analyses and writing.

III Salonen, K, Järvinen, H, Eresmaa, R and S Niemelä, 2007: Bias estimation of Doppler-radar radial-wind observations. *Quarterly Journal of the Royal Meteorological Society*, **133**: 1501–1507.

PAPER III discusses some special aspects related to the bias estimation for Doppler radar radial wind observations. Calculating the bias in the conventional way by summing up the observation minus background values can give a zero result even when there are systematic differences in the wind speed and/or direction. A bias estimation method designed for this observation type is introduced in the paper. The author is the primary contributor to the article, including the bias estimation method development, coding, testing, and also most of the analyses and writing.

IV Salonen, K, Järvinen, H, Järvenoja, S, Niemelä, S and R Eresmaa, 2008: Doppler Radar Radial Wind Data in NWP model validation. *Meteorological Applications*, **15**: 97–102.

PAPER IV investigates the possibility of exploiting Doppler radar radial wind observations in NWP model validation. Two versions of the HIRLAM model, which differ only in the formulation of the surface stress direction, are validated over a period of one month. The observation minus background statistics advocate the use of high-resolution radar data as model validation material. It is demonstrated that subtle differences in model versions due to different parameterization details can be distinguished with high statistical confidence. The author is responsible for all the experimentation, as well as most of the analyses and writing.

1 INTRODUCTION

Numerical weather prediction (NWP) models provide the basis for modern weather forecasting by simulating the evolution of the atmospheric state. NWP models are based on a set of governing equations which describe the evolution of atmospheric variables, such as pressure, temperature, wind, and humidity. The first attempt to predict the weather numerically was made by Richardson (1922). The forecast failed spectacularly due to imbalances between initial winds and initial pressures (Lynch, 2006). The history of the computer-based NWP dates back to the beginning of the 1950's (Charney and Eliassen, 1949; Charney et al., 1950). The accuracy of NWP models has improved considerably during recent decades due to improved observational networks, increased computing power and the development of sophisticated methods for numerical modelling and for determining the initial state for the NWP model, i.e., data assimilation (e.g. Shuman, 1989; Untch et al., 2001).

The atmospheric phenomena that the NWP models simulate occur on many different spatial and temporal scales (e.g. Daley, 1991). These range from large planetary-scale systems down to small microscale phenomena. Planetary-scale atmospheric phenomena extend over several thousand kilometres and last from several days to weeks. Synoptic-scale phenomena, such as the high and low pressure systems in midlatitudes, occur on scales from several hundred kilometres to several thousand kilometres and have a time-span of days to a week. Mesoscale phenomena including convective systems and topographically-generated weather systems, such as mountain waves and sea and land breezes, have a spatial scale of the order of a few to several hundred kilometres and a time scale from hours up to a day. The finest-scale models also aim to simulate microscale phenomena such as turbulent eddies and individual cumulus clouds.

NWP models can be roughly divided into two types. Global models are typically used for medium-range forecasts, i.e., for $\sim$ 2 - 15 day forecasts; in these, the main focus is on forecasting global and synoptic-scale phenomena. Limited area models can be run with a higher spatial resolution than global models, and are used for more detailed forecasts and for shorter time ranges, typically from about 3-hour to 2-day forecasts. In present-day limited area models the horizontal resolution is of the order of 2 – 10 km. Limited area models are not self-contained; they require lateral boundary conditions at the borders of the model domain. These lateral boundary conditions are typically obtained from a global model or from a coarser resolution limited area model that has a larger model domain (e.g. Kalnay, 2003).

The time integration of an NWP model is an initial-value problem, i.e., a good forecast requires the initial state of the atmosphere to be known accurately, and the NWP model to be a realistic representation of the atmosphere. Data assimilation methods are used to produce the initial conditions for NWP models. In data assimilation, the model background field, which is typically a short-range forecast, is updated with available observations in a statistically optimal way. The estimate of the state of the

atmosphere so obtained is called the analysis.

Various kind of observations are exploited when producing the analysis for an NWP model. Radiosonde observations which provide measurements of temperature, pressure, humidity, and wind at different altitudes are still the most important source of information for NWP models (Bouttier and Kelly, 2001). In addition, surface synop observations, ship and buoy observations as well as aircraft observations provide useful in situ measurements for NWP models. However, the observation network for these conventional observations is spatially and temporally sparse and irregularly distributed. To overcome these limitations, conventional observations can be augmented by remote sensing observations, such as those from satellites and radars (e.g. Ohring et al., 2002; Eresmaa et al., 2008; Alberoni et al. 2001). Typically, remote sensing observations have an excellent spatial and temporal resolution. However, remote sensing observations are usually not of model variables as such, and observation modelling is required.

For extra-tropical synoptic-scale motions the horizontal velocities are approximately geostrophic, i.e., the coriolis force and the horizontal pressure-gradient force balance each other (e.g. Holton, 1992). Thus, for a synoptic-scale NWP, the accurate initial condition of the mass-wind balanced flow is essential for acceptable forecast quality. For a mesoscale NWP, accurate initial conditions for both the balanced and the unbalanced parts of the wind field are essential to generate forecasts of acceptable quality. For these scales, the theory of geostrophic adjustment (Rossby, 1938) implies that wind observations are necessary for determining the state of the atmosphere (Kalnay, 1985). This sets an additional requirement for mesoscale observing networks: high spatial and temporal resolution observations are necessary, wind observations in particular being important.

Doppler radar winds are one potential source of wind observations for mesoscale NWPs (e.g. Sun and Crook, 1997; Alberoni et al. 2001; Lindskog et al. 2004; Seko et al. 2004; Xiao et al. 2005; Montmerle and Faccani, 2008). In many countries, as also in Finland, the Doppler weather radar network has a good geographical coverage and radial wind velocity measuring capability.

The objective of this thesis has been to develop and exploit data assimilation tools for Doppler radar radial wind observations. The work has been carried out in the High Resolution Limited Area Model (HIRLAM; Undén et al., 2002) framework, using a three-dimensional variational data assimilation system (3D-Var; Gustafsson et al., 2001; Lindskog et al., 2001). This thesis consists of an introductory part and of four peer-reviewed articles. The key questions considered in PAPERS I – IV included in this thesis are:

- How should one model Doppler radar radial wind observations? What are the main aspects to be taken into account, and what are their relative importances? (PAPER I)

- How and why should the raw radial wind observations be preprocessed prior to data assimilation? (PAPER II)

- What are the special features of radar radial wind observations, and how should they be taken into account in bias estimation? (PAPER III)
- Could radar radial wind observations be of additional value in NWP model validation? (PAPER IV)

The introductory part of this thesis is organised as follows: Chapter 2 discusses numerical weather prediction by providing an overview of the governing equations of the atmosphere and data assimilation. Chapter 3 introduces the Doppler radar radial wind measurement and the related error characteristics. Chapter 4 presents the main results from PAPERs I – IV. Conclusions are drawn in Chapter 5.

2 BASIC CONCEPTS OF NUMERICAL WEATHER PREDICTION

A numerical weather prediction system consists of two main components: a forecast model and a data assimilation system. The former consists of the physical description of the atmosphere, whereas the latter is used to produce the initial conditions for the forecast model.

2.1 GOVERNING EQUATIONS AND PHYSICAL PARAMETERIZATIONS

The evolution of the atmospheric state can be described with a set of partial differential equations (e.g. Pielke, 2002):

$$\frac{\partial \rho}{\partial t} = -(\nabla \cdot \rho \vec{V}) \tag{2.1}$$

$$\frac{\partial \theta}{\partial t} = -\vec{V} \cdot \nabla \theta + S_\theta \tag{2.2}$$

$$\frac{\partial \vec{V}}{\partial t} = -\vec{V} \cdot \nabla \vec{V} - \rho^{-1} \nabla p - g\vec{k} - 2\vec{\Omega} \times \vec{V} \tag{2.3}$$

$$\frac{\partial q_n}{\partial t} = -\vec{V} \cdot \nabla q_n + S_{q_n}, \qquad n = 1, 2, 3 \tag{2.4}$$

$$\frac{\partial \chi_m}{\partial t} = -\vec{V} \cdot \nabla \chi_m + S_{\chi_m}, \qquad m = 1, 2, \ldots, M \tag{2.5}$$

Equations 2.1 – 2.5 represent the conservation laws of mass, heat, motion, water, and other gaseous and aerosol materials, respectively. In the equations above, ρ is density, t is time, $\vec{V}$ is the 3-dimensional wind vector, θ is potential temperature, p is pressure, $-g\vec{k}$ is gravitational acceleration, $\vec{\Omega}$ is the angular velocity of the Earth's rotation, q_n is the mass ratio between each of the water phases and air, and χ_m is the mass ratio between any chemical species, except water, and air. S_θ, S_{q_n}, and S_{χ_m} are the source-sink terms of heat, water, and other chemical species, respectively.

Typically these equations are simplified to some degree in NWP models. One of the most common simplifications is the hydrostatic approximation, i.e., the vertical acceleration term ($\frac{\partial \omega}{\partial t}$) is neglected in the equation of conservation of motion, 2.3. The hydrostatic approximation requires that the vertical acceleration is small compared with the gravitational acceleration. Scale analysis shows that the hydrostatic approximation is valid as long as the horizontal extent of the circulation is larger than its vertical counterpart (e.g. Holton, 1992). To represent small-scale phenomena, such as convective clouds or storms, in an NWP model, it is necessary to use the equation of motion without the hydrostatic approximation. The HIRLAM model utilised in this thesis is a hydrostatic NWP model.

The non-linear partial differential equations 2.1 – 2.5 are discretized over finite spatial and temporal scales, and solved using numerical techniques. The solution of the

equations is an initial-value problem, i.e., initial fields of mass and velocity are required to obtain the mass and velocity distribution at some future time. Because of the non-linearity of the equations, small errors in the initial conditions will grow in time, and thus the accuracy of the solution will degrade in time (e.g. Thompson, 1957; Lorenz, 1965; Palmer, 1993).

For the discretization, all the dependent variables in 2.1 – 2.5 are de-composed as

$$\phi = \overline{\phi} + \phi', \tag{2.6}$$

where ϕ is any one of the dependent variables (Pielke, 2002). In 2.6 $\overline{\phi}$ represents the spatial average over a grid-box, and ϕ' the subgrid-scale perturbations around the averaged state. Discretization is applied to all variables in 2.1 – 2.5. A grid-box average, which is linear in the perturbations, is zero by definition, i.e. $\overline{\phi'} = 0$ and $\overline{\overline{\phi}\phi'} = 0$. The averaged terms, $\overline{\overline{\phi}\ \overline{\phi}} = \overline{\phi\phi}$, are resolved explicitly by the model dynamics, while the subgrid-scale correlation terms, $\overline{\phi'\phi'}$, must be parameterized as a function of the grid-averaged variables. These parameterizations constitute the model physics.

The model parameterizations comprise the radiation processes and subgrid-scale transport of the dependent variables, such as momentum, heat, and moisture down to the small scales associated with turbulence. The thermodynamics associated with latent heat release, such as condensation, evaporation, sublimation, and precipitation, as well as the surface, soil and orography related processes must also be parameterized (e.g. Pielke, 2002; Kalnay, 2003).

2.2 DATA ASSIMILATION

As discussed in the previous section, the solution of the governing equations is an initial-value problem. Talagrand (1997) has defined the purpose of data assimilation as the use of all the available information to determine the state of the atmospheric or oceanic flow as accurately as possible.

The initial conditions for an NWP model are produced through a statistical combination of the model background state $\mathbf{x_b}$, which is typically a short-range forecast from the previous analysis, and of the observations $\mathbf{y}$ (e.g. Lorenc, 1986). The analysis $\mathbf{x_a}$ obtained with the least-squares estimation method is defined as follows:

$$\mathbf{x_a} = \mathbf{x_b} + \mathbf{K}(\mathbf{y} - H\mathbf{x_b}) \tag{2.7}$$

$$\mathbf{K} = \mathbf{B}\mathbf{H^T}(\mathbf{H}\mathbf{B}\mathbf{H^T} + \mathbf{R})^{-1} \tag{2.8}$$

In 2.7, H is the observation operator which produces the model counterpart for the observed quantity, and $\mathbf{K}$ is the optimal gain matrix. In 2.8 $\mathbf{B}$ and $\mathbf{R}$ are the error covariance matrices for the model background and for the observations, respectively. $\mathbf{H}$ is the tangent linear observation operator, and $\mathbf{H^T}$ its transpose, which is called the adjoint of the observation operator. The resulting analysis is a minimum variance estimate, i.e., the analysis state is as close as possible to the true state in the rms sense.

In the derivation of the analysis equation, the following assumptions are made:

- The tangent linear hypothesis, $H(\mathbf{x}) - H(\mathbf{x_b}) = \mathbf{H}(\mathbf{x} - \mathbf{x_b})$, is valid. This means that the variations of the observation operator in the vicinity of the background state are linear.
- The observation and the background errors are uncorrelated with each other.
- The expectation of the background errors and the observation errors is zero.
- The observation and the model background error covariance matrices are positively definite.

There are two alternative approaches to solve the analysis equation 2.7: to directly compute the gain matrix $\mathbf{K}$, or to search for an approximate solution by minimisation of a cost function which is proportional to the square of the distance between the model state and both the background and the observations. The former approach leads to data assimilation techniques such as optimal interpolation (Gandin, 1963), Kalman filtering (Kalman, 1960) and its modifications such as fast Kalman filtering (Lange, 2001) and reduced rank square-root Kalman filtering (Veerlan and Heemink, 1997). The latter approach, on the other hand, leads to 3-dimensional and 4-dimensional variational data assimilation methods (e.g. Lewis and Derber, 1985; Lorenc, 1986; Courtier and Talagrand, 1990). The analysis method in the HIRLAM model versions utilized in this thesis is 3-dimensional variational data assimilation (Gustafsson et al., 2001; Lindskog et al., 2001).

The major difference between Kalman filtering based data assimilation algorithms and other data assimilation algorithms is that in Kalman filtering the forecast error covariance is advanced in time by the model, instead of estimating the error covariances with a constant background error covariance matrix $\mathbf{B}$. However, Kalman filtering is computationally very expensive and is thus often impractical for use in operational NWP models. A widely-used simplification of Kalman filtering is the ensemble Kalman filtering technique (Evensen, 1994; Houtekamer and Mitchell, 1998). In this approach an ensemble of n data assimilation cycles is made, and the ensemble is used to estimate the forecast error covariance matrix.

Variational data assimilation

In variational data assimilation the direct computation of the gain matrix $\mathbf{K}$ is avoided. In 3-dimensional variational data assimilation (3D-Var), the analysis is obtained by minimising a cost function

$$\begin{aligned} J &= J_b + J_o \\ &= \frac{1}{2}(\mathbf{x} - \mathbf{x_b})^{\mathbf{T}}\mathbf{B^{-1}}(\mathbf{x} - \mathbf{x_b}) + \frac{1}{2}(H\mathbf{x} - \mathbf{y})^{\mathbf{T}}\mathbf{R^{-1}}(H\mathbf{x} - \mathbf{y}). \end{aligned} \tag{2.9}$$

In 2.9, the term J_b measures the distance between the model state $\mathbf{x}$ and the model background state $\mathbf{x_b}$, while the term J_o measures the distance between the model state and

the observations $\mathbf{y}$. The solution is sought by using iterative methods and performing several evaluations of the cost function and its gradient

$$\nabla J \;=\; \mathbf{B^{-1}}(\mathbf{x}-\mathbf{x_b}) - \mathbf{H^T R^{-1}}(\mathbf{y}-H\mathbf{x}). \tag{2.10}$$

4-dimensional variational data assimilation (4D-Var) is a generalisation of 3D-Var, and takes into account the exact observation time. The cost function is similar to 2.9, but the observation operators are generalised to include a forecast model that will allow a comparison between the model state and the observations at the appropriate time.

In operational implementations the cost function is often implemented in its incremental form (Courtier et al., 1994), where the full resolution assimilation increment $\delta\mathbf{x} = \mathbf{x} - \mathbf{x_b}$ is represented at a lower horizontal resolution than the full model state. The use of the incremental form is an efficient way of reducing computational demands.

The advantage of the variational data assimilation is its relatively straightforward way of exploiting indirect observations of the NWP model variables, such as satellite infrared radiances (e.g. Eyre, 1990), GPS zenith total delays and slant delays (e.g. Vedel and Huang, 2004; Eresmaa and Järvinen, 2006), radar reflectivities (e.g. Caumont et al., 2006a), and Doppler radar radial winds (e.g. Lindskog et al., 2004; Sun and Crook, 1997, Seko et al., 2004). A common factor in the exploitation of these data types is the observation modelling. The observed quantities are expressed in terms of the model variables with the observation operator H. In addition, the tangent linear and the adjoint of the observation operator needs to be provided.

3 DOPPLER RADAR RADIAL WIND MEASUREMENT

3.1 MEASUREMENT PRINCIPLE

A Doppler radar emits electromagnetic pulses which backscatter from atmospheric hydrometeors. The scattering hydrometeors are in three-dimensional motion. The radial velocity, v_r, of these hydrometeors can be determined from the phase shift between the back-scattered returns from successive radar pulses (e.g. Doviak and Zrnić, 1993)

$$v_r = \frac{\lambda}{4\pi}\frac{\Delta\Phi}{\Delta t}. \tag{3.1}$$

In 3.1 λ is the radar wavelength, $\Delta\Phi$ is the phase difference, and Δt is the time difference between successive radar pulses.

Typically, the number of the scattering hydrometeors in a radar pulse volume is large, and the distribution of their velocity can be approximated by a continuous distribution (Sauvageot, 1992). The power-weighted velocity distribution of the back-scattered signal is called the Doppler spectrum. The power weight depends on the scatterers' reflectivity and in addition also on the weights given to the scatterers by the radiation pattern, the transmitted pulse shape, and the receiver's response to it. The average radial velocity in the radar pulse volume is the moment of order 1 of the Doppler spectrum.

Shape of the radar pulse volume

The volume of the emitted radar pulse broadens with increasing measurement range in the horizontal and vertical directions. The shape of the radar pulse volume is determined by the radar antenna radiation pattern. Most of the energy in the radiation pattern is concentrated in the main lobe and in addition, several side lobes exist. The width of the main lobe is defined as containing half the power of the maximum radiation on the pulse path axis, i.e., -3 dB. The main lobe contains more than 80% of the total energy transmitted by the antenna. The power distribution in the radar pulse main lobe is approximately Gaussian (Probert-Jones, 1962).

The radar pulse volume shape remains unchanged in the radial direction as the pulse propagates away from the antenna. The power distribution in the radial direction is determined by the pulse shape, the receiver impulse response, and the processing performed in the radar signal processor.

3.2 RANGE-VELOCITY AMBIGUITY PROBLEM

Interpretation of the Doppler radar radial wind measurements is complicated by the range-velocity ambiguity problem (Doviak and Zrnić, 1993). Doppler radar measurements are often made with a constant pulse repetition frequency (PRF). In that case, the

maximum unambiguous range r_{max} for radar measurements is

$$r_{max} = \frac{c}{2 \cdot \text{PRF}}. \tag{3.2}$$

Thus, echoes for the transmitted pulse n from scatterers located at a range longer than the maximum unambiguous range are received in the same time interval as echoes for the transmitted pulse $n + 1$ from ranges shorter than r_{max}. This means that the range r to a distant scatterer may appear to have a value of $r' = r - (N - 1)r_{max}$, where N designates the number of r_{max} intervals to the scatterer. In 3.2 c is the speed of light.

The other ambiguity relates to the scatterer's velocity measurement. If the radial velocity is such that the phase difference between the successive pulses is greater than π radians, there is an ambiguity concerning the measurement of the phase and, therefore, the measurement of the radial wind. The maximum radial velocity v_{max} that can be measured unambiguously is

$$v_{max} = \frac{\lambda \cdot \text{PRF}}{4}. \tag{3.3}$$

The pulse repetition frequency PRF appears in both equations 3.2 and 3.3. Thus, the maximum unambiguous velocity v_{max} and the maximum unambiguous range r_{max} are related to each other through

$$v_{max} r_{max} = \frac{\lambda c}{8}. \tag{3.4}$$

The product of the maximum values of the velocity and the range is a constant which depends on the radar wavelength λ. For example, for a C-band radar operating with a wavelength of 5.7 cm, a maximum unambiguous range of 200 km results in an unambiguous velocity interval of only $\pm$10.7 ms^{-1}. The choice of r_{max} and v_{max} is always some kind of a compromise in operational radar measurements.

Various measurement techniques, such as dual-PRF (Dazhang et al., 1984), staggered pulse repetition time (Sirmans et al., 1976) and Simultaneous Multiple Pulse Repetition Frequency code (Pirttilä et al., 2005) have been developed to decrease the limitations caused by the range-velocity ambiguity problem. The measurements can also be postprocessed by using so-called dealiasing algorithms (e.g. Ray and Ziegler, 1977; Haase and Landelius, 2004). Alleviating the range-velocity ambiguity problem is a continuous research topic in radar meteorology.

3.3 Other error sources

There are several other sources of errors that affect the accuracy of the radar radial wind measurements besides the range-velocity ambiguity problem. These can be divided into instrumental errors and misinterpretation of echoes from non-meteorological targets, i.e., clutter.

Instrumental errors consist of fluctuations in the stability of the electronics, signal processing accuracy, antenna accuracy and possible electromagnetic interference

caused, e.g., by other radars (Michelson et al., 2004). Instrumental errors can be both random and systematic. Systematic errors, such as the orientation accuracy of the radar antenna, can be decreased effectively by careful maintenance of the radar. The impact of the random part of the instrumental errors can be minimised by super-observation processing, as will be discussed in section 4.2.

Clutter is caused by non-meteorological scatterers such as birds, insects, sea, and ground. Clutter can be identified and removed with various kinds of postprocessing methods (e.g. Larkin, 1991; Gabella and Notarpietro, 2002; Peura, 2002). In this thesis it is assumed that the radar observations are free of clutter.

4 MAIN RESULTS

In the following sections, the main results of this thesis are covered. The results of PAPERS I, II, III, and IV are discussed in Sections 4.1, 4.2, 4.3, and 4.4, respectively.

4.1 MODELLING OF THE OBSERVATIONS

Observation modelling is a key element in exploiting indirect observations of the NWP model variables. PAPER I considers the observation operator development for radar radial wind observations and builds on earlier work presented in Lindskog et al. (2000) and Lindskog et al. (2004). The purpose of the observation modelling is to express the observed radar radial wind component in terms of the model horizontal wind vector at the observation location.

The observation operator for Doppler radar radial winds includes the following three steps:

1. The NWP model profiles of the horizontal wind components u and v are interpolated to the observation location.

2. The interpolated wind components are projected on the horizontal plane towards the radar using
$$v_h = u \sin\theta + v \cos\theta, \tag{4.1}$$
where θ is the azimuth angle of the radar measurement.

3. v_h is projected on the vertical plane to the slanted direction towards the radar using
$$v_r = v_h \cos(\phi + \alpha), \tag{4.2}$$
where v_r is the radar radial wind component and ϕ is the radar antenna elevation angle.

In 4.2, the argument α approximately takes into account the curvature of the Earth through the formula

$$\alpha = \arctan\left(\frac{d\cos\phi}{d\sin\phi + \frac{4}{3}r + h}\right), \tag{4.3}$$

where h is the height of the radar antenna above mean sea level, d is the measurement range, and r is the radius of the Earth (Doviak and Zrnić, 1993).

In the formulation of the observation operator, it is assumed that the fall speed of hydrometeors is not observed. This assumption is made in 4.1 where only the NWP model horizontal wind is included. The assumption is justified for assimilation of

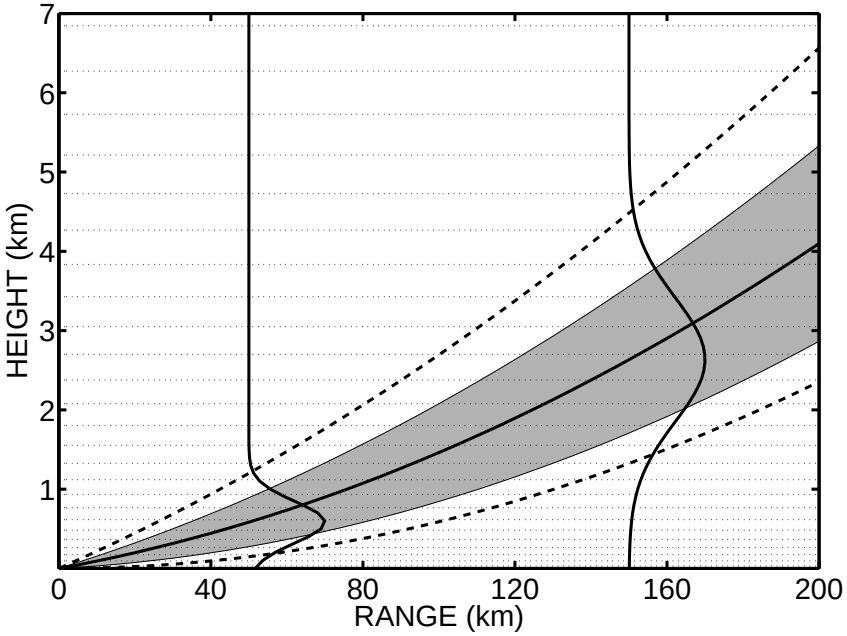

FIGURE 4.1. An illustration of the radar pulse volume broadening with a 0.7° two-way beamwidth (shaded area), the radar horizon and the upper limit for the Gaussian averaging kernel (dashed lines), and the shapes of the averaging kernel at measurement ranges of 50 km and 150 km. The dotted horizontal lines represent the HIRLAM model levels. The radar antenna elevation angle is 0.5°. (Figure 3 of PAPER I)

Doppler radar radial wind measurements at low elevation angles, i.e., elevation angles, at which the projection of the vertical wind component on the radar pulse path can be assumed to be negligible.

The horizontal interpolation is performed with bi-linear interpolation in step 1. of the observation operator. In the basic version of the observation operator, the vertical interpolation is done with a linear interpolation, i.e., as a convolution between a full model wind profile and a "hat" function which peaks at the observation height, and has a width of two model levels.

However, the radar radial wind velocity is not a point measurement, but rather a weighted average over the radar pulse volume, as described in Section 3.1. Figure 4.1 illustrates the vertical pulse volume broadening as a function of measurement range. In the first refinement of the observation operator, the hat function is replaced with a Gaussian averaging kernel

$$w \;=\; \exp(-\ln 2\frac{(z-z_0)^2}{\kappa}) \tag{4.4}$$

in the vertical interpolation. In 4.4 z is the model level height and z_0 is the observation height. The argument κ

$$\kappa \;=\; (z_k - z_0)^2 \tag{4.5}$$

defines the width of the kernel. In 4.5 z_k is the height of the upper limit of the volume half-power width, calculated with the so-called $\frac{4}{3}r$ -law at measurement range d. The $\frac{4}{3}r$ -law assumes the standard atmospheric refraction conditions of the so-called ICAO standard atmosphere (Doviak and Zrinić, 1993). The obscuring effect of the radar horizon is taken into account by assuming a radar horizon of 0° elevation angle, while an empirical upper bound is set to a height of 1.5 times the volume half-power width. Outside these bounds the model information is not used in the vertical interpolation. Examples of the vertical averaging kernel at ranges of 50 km and 150 km are shown in Fig. 4.1. The dotted horizontal lines represent the HIRLAM model levels. It can be clearly seen that the radar pulse volume extends over several model levels in the vertical, especially at longer measurement ranges.

The radar pulse volume broadens in the horizontal and in the vertical directions in the same way. The horizontal resolution of the NWP model determines whether the horizontal broadening of the pulse volume has to be taken into account. A bi-linear horizontal interpolation is expected to be accurate enough if the horizontal extent of the pulse volume is small compared to the NWP model grid cell.

The second refinement of the observation operator concerns modelling of the radar pulse path bending. Typically the observation height at range d is obtained with the $\frac{4}{3}r$ -law. The actual local refraction index in the NWP model atmosphere can be calculated from the NWP model temperature, pressure, and water vapour partial pressure profiles. The radar pulse path bending in the NWP model atmosphere is then obtained by applying Snell's law. Modelling the pulse path bending has two effects: the observation height at range d is different from that obtained with the $\frac{4}{3}r$ -law, and the effective elevation angle of the radar pulse path is different from the antenna elevation angle.

A one-month model experiment for January 2002 has been performed to validate the basic version of the observation operator and the two refinements. The general conclusion of the validation is that modelling of the Doppler radar volume broadening improves the accuracy of the observation operator. The impact of using the Gaussian averaging kernel in the vertical interpolation is largest when there is a local maximum or minimum in the wind profile near the observation height. Modelling of the pulse path bending operates mainly through changes in the observation height, and only to a minor extent through changes in the effective elevation angle. Modelling of the pulse path bending has on average a negligible impact on the observation minus model background (OmB) bias and standard deviation statistics.

4.2 PROCESSING OF THE OBSERVATIONS FOR DATA ASSIMILATION

Observation processing is another key element in exploiting radar radial wind observations in NWP models. PAPER II considers this aspect. A benefit of the variational data assimilation, combined with the observation modelling, is that the conversion of the observations into the NWP model variables is avoided. In the case of radar radial

wind observations some preprocessing is, however, necessary to reduce the enormous amount of raw observations before they are introduced into the data assimilation system.

The radar radial wind observation operator is accurate, apart from three types of error:

- Instrumental errors, such as errors in the radar calibration.
- Modelling errors, such as numerical errors, and errors in the observation modelling.
- Representativeness errors, which are due to the model's incapability to describe the observed phenomena with its limited physics or dynamics, or due to insufficient resolution of the model discretization.

All of the above-described error types consist of a systematic and a random part. The random part of the instrumental and representativeness errors can be effectively decreased by computing a spatial mean from a small number of raw observations. The concept of a so-called super-observation was first introduced by Lorenc (1981). Super-observations are spatial averages and can be thought to better represent the scales described by the NWP model. Super-observation generation methods have been applied to conventional observation types (e.g. Lorenc, 1981; Lönnberg and Shaw, 1983), and for remote sensing observations such as atmospheric motion vectors (Berger et al., 2004), satellite soundings of temperature and moisture (Hart et al., 1993), and radar radial winds (e.g. Albers, 1995; Xiao et al., 2003; Lindskog et al., 2004; Seko et al., 2004; Swarbrick, 2006).

A fundamental question concerning super-observation generation is, what is the optimal size for the spatial averaging area? The random errors of the resulting super-observations are small when a large averaging area is used. However, observations may represent different atmospheric phenomena if they originate too far apart from each other. On the other hand, a small averaging area ensures that the observations represent the same atmospheric phenomena but it may not be large enough to reduce the impact of random errors.

In the HIRLAM approach to super-observation (hereafter SO) generation, the averaging area and the spacing of the SOs are determined by two free parameters, the azimuthal averaging $\overline{\phi}$ and the range bin spacing $\overline{R}$. A schematic illustration of the SO generation is shown in Fig. 4.2. The SO generation algorithm is designed so that fewer raw observations are used in the SO near the radar than at longer measurement ranges. In practice, the size of the averaging area of an SO is usually defined with the parameter $\overline{\phi}$, and the range spacing with $\overline{R}$. Thus, the choice of the parameter $\overline{\phi}$ impacts mainly on averaging out the random errors, and the choice of the parameter $\overline{R}$ has a thinning effect on the data in the radial direction.

In PAPER II the SO processing has been experimentally optimized. The impact of varying both SO generation parameters has been studied with HIRLAM horizontal

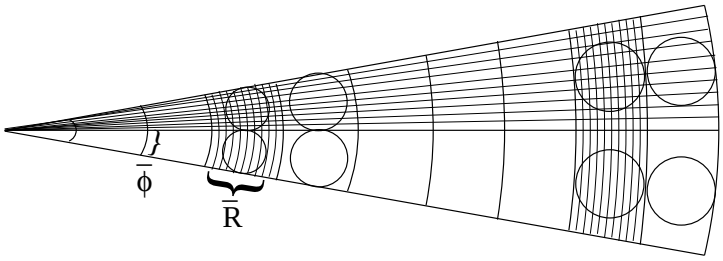

FIGURE 4.2. A schematic illustration of the HIRLAM approach to super-observation generation. Parameter $\overline{R}$ defines the range bin spacing and parameter $\overline{\phi}$ defines the azimuthal averaging. (Figure 1 of PAPER II)

model resolutions of 5.5 km, 11 km, and 22 km. The resolution of the raw radar radial wind observations is 1 km in range and 420 azimuth gates per 360° scan, resulting in a $\sim$0.9° azimuthal resolution. The viewpoint is that the impact of the random instrumental errors can be minimised by optimizing the super-observation processing. The impact of the random representativeness errors may also be decreased to some extent, as super-observations better represent the scales of the NWP model. However, removal of the impact of the random modelling errors is thought to be beyond the capabilities of the super-observation processing.

Results from the model experiments with SO data sets, where $\overline{\phi}$ has a constant value and $\overline{R}$ varies, indicate that the OmB vector wind bias at measurement ranges shorter than 10 km is notably larger for an $\overline{R}$ value of 5 km than for $\overline{R}$ values of 10 km and 20 km. This is due to the fact that at short ranges radar measurements are contaminated with ground clutter, as the lower part of the radar pulse volume may be reflected from the ground, buildings etc. The SO data set in which $\overline{R} = 5$ km includes notably more of these erratic measurements than the other two SO data sets. The bias and the standard deviation are at the same level for all three SO data sets, if observations from measurement ranges shorter than 10 km are excluded. Thus the choice of the parameter $\overline{R}$ is not very critical, affecting mainly the data amounts. Using $\overline{R} = 5$ km ($\overline{R} = 20$ km) doubles (halves) the data amount compared to using $\overline{R} = 10$ km. A constant value of 10 km for $\overline{R}$ has been used in the experiments where varying values for $\overline{\phi}$ are studied. The choice can be justified as the SO data sets are large enough for reliable bias estimation and the data handling is convenient.

Figure 4.3 illustrates the OmB vector wind bias as a function of the parameter $\overline{\phi}$. Raw observations thinned to a 10 km range resolution are also considered. This data set is marked in Fig. 4.3 as 'RAW'. The vector wind bias is the smallest for the thinned raw data, and the bias increases with increasing $\overline{\phi}$. This is valid for all model resolutions. In the data sets studied, the wind speed bias is dominant over the wind direction bias, and the vector wind bias behaves in a similar manner to the wind speed bias.

The increase in the wind speed bias as a function of $\overline{\phi}$ may be partly explained by

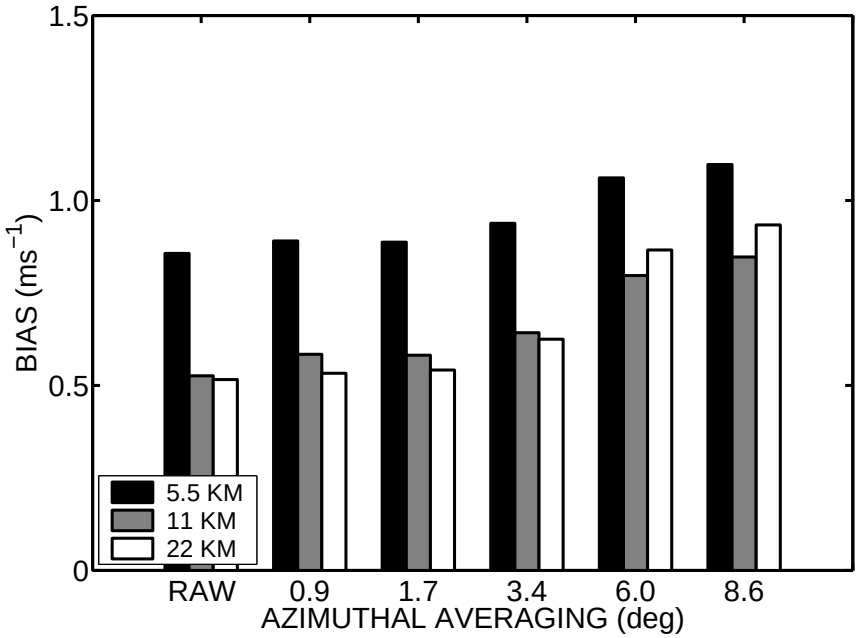

FIGURE 4.3. Vector wind bias shown as a function of azimuthal averaging ($\overline{\phi}$) used in the SO generation. The thinned raw data is marked with 'RAW'. Black bars indicate the 5.5 km model run, gray bars the 11 km model run, and white bars the 22 km model run. (Figure 7 of PAPER II)

the fact that using a wide $\overline{\phi}$ in the SO processing reduces the maximum (towards and away from the radar antenna) wind speeds. However, theoretical considerations applied to a uniform and linear wind field show that the bias introduced by azimuthal averaging is extremely small. Thus, it is unlikely that the reduction in maximum wind speeds due to averaging in azimuth direction could alone explain the increase in the wind speed bias. The increase in the bias can be significantly stronger if ground clutter is present in the raw data. Thus, the increase of the bias as a function of $\overline{\phi}$ seen in Fig. 4.3 may be a consequence of remaining clutter, even though clutter removal has been performed prior to the SO processing.

Figure 4.4 displays the OmB standard deviation of the radar radial wind component as a function of $\overline{\phi}$. The OmB standard deviation decreases until it reaches a minimum at SOs generated with a value of 3.4° for $\overline{\phi}$, and increases again for the larger $\overline{\phi}$. The behaviour is similar for all three model resolutions considered. This implies that generating SOs with a large averaging area decreases random errors effectively to a certain point. However, too wide a $\overline{\phi}$ degrades the quality of the SOs.

Based on the model experiment results, PAPER II recommends the use of a $\overline{\phi}$ value of the order of 0.9° – 1.7°. In more general terms, the recommended parameter value $\overline{\phi}$=1.7° corresponds to a 1.7 km^2 averaging area at a 50 km measurement range, and a 7.3 km^2 averaging area at a 100 km measurement range.

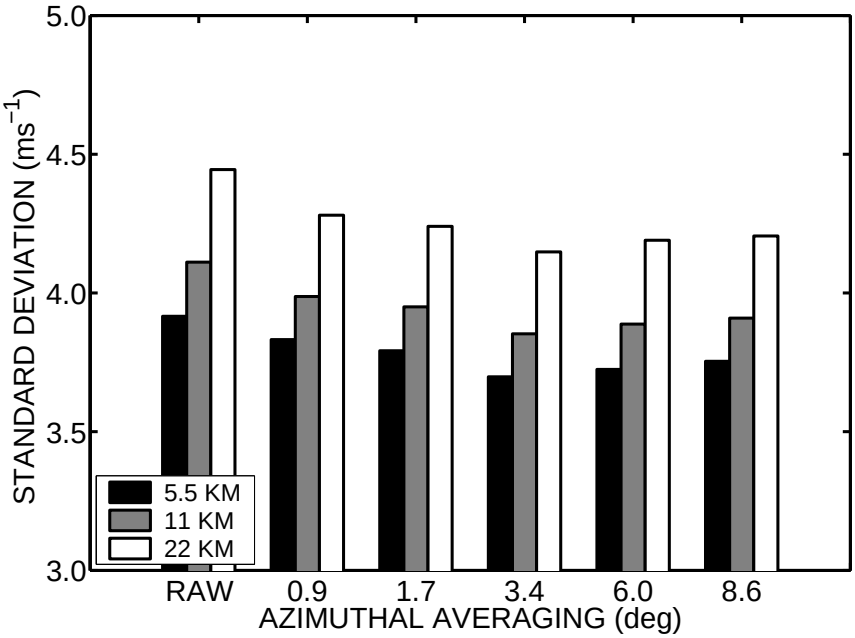

FIGURE 4.4. As Fig. 4.3 but for observation minus model background standard deviation of the radar radial wind component. (Figure 9 of PAPER II)

4.3 BIAS ESTIMATION METHOD

PAPER III [1] introduces a bias estimation method specially designed for Doppler radar radial wind observations. The bias estimation method has been applied in the analysis of the model experiment results in PAPER I, PAPER II, and PAPER IV.

Doppler radar measures the radial wind component by azimuthal scanning through 360°. In the case of a uniform wind field, the radial wind component has a cosine form as a function of azimuth angle at a given elevation and range. The amplitude of the cosine function determines the wind speed, and its phase determines the wind direction (e.g. Sauvageot, 1992). Aggregation of the radar radial wind OmB values for different azimuth directions in the bias calculation can result in a zero bias, even in the presence of systematic differences in the observed and modelled wind speed and/or direction. This is due to the symmetric nature of the radial wind component as a function of azimuth angle.

The Doppler radar radial wind bias estimation method presented in PAPER III enables presenting the systematic differences between the radar radial wind observations and their model counterparts in terms of wind speed and direction biases. The bias estimation method includes the following steps.

1. A reference direction is chosen to make the radial wind observations comparable

[1] After PAPER III was published, an error was found in the super-observation processing software. The super-observations utilised have been generated using an azimuthal averaging of 3.4° instead of 1.7°. This does not affect the interpretation of the results.

with each other.

2. A rotation angle $\Delta\phi$ is determined as a difference between the reference wind direction and the model wind direction. The azimuth angle corresponding to the observation is rotated by adding $\Delta\phi$ to it.

3. After the rotation, an azimuth bin average is calculated. By fitting the radial wind equation $v_r = v_h \cos(\delta - \phi)$ to the bin-averaged observations, estimates for horizontal wind speed v_h and direction $\delta + \pi$ are obtained.

The steps of the bias estimation method are illustrated in Fig. 4.5. The top panel of Fig. 4.5 shows ca. 16 300 radial wind observations as a function of azimuth angle from four different radars on 31 January 2002 at 12 UTC. Different wind directions are represented in the data set. In this illustration the reference direction is chosen to be 180°, i.e., South (step 1). The middle panel of Fig. 4.5 shows the radial wind observations after the rotation (step 2). The general shape of the cloud of points indicates a southerly wind direction due to the rotation. The bottom panel of Fig. 4.5 shows the bin-averaged radial wind speed (black dots) and the fitted radial wind curve (black solid line) (step 3). In this data set, the mean observed wind speed is 9.3 ms^{-1} from 173°.

The above-described procedure is also applied to the model counterparts of the observations. The differences in the amplitude and phase of the fitted v_r curves indicate biases in the wind speed and direction, respectively. In the case of the data set shown in Fig. 4.5, the mean model background wind speed is 9.4 ms^{-1} from 180°. Thus, there is a 0.1 ms^{-1} bias in the wind speed and a 7° bias in the wind direction.

The functioning of the bias estimation method has been demonstrated with a one-month data set in PAPER III. A more extensive evaluation of the applicability of Doppler radar radial wind observations in NWP model validation is presented in PAPER IV.

4.4 DOPPLER RADAR RADIAL WIND OBSERVATIONS IN NWP MODEL VALIDATION

The tools developed for data assimilation of indirect observations of the NWP model variables can also be used to exploit the observations for NWP model validation (e.g. Rikus, 1997; Niemelä and Fortelius, 2005; Caumont et al., 2006b). PAPER IV [1] investigates the potential of exploiting Doppler radar radial wind observations in NWP model validation. The study makes use of both the developed radar radial wind observation operator (PAPER I), and the radar radial wind bias estimation method (PAPER III).

A HIRLAM surface stress parameterization detail which affects the boundary layer winds in a systematic manner offers an interesting framework for the validation

[1] After PAPER IV was published, an error was found in the super-observation processing software. The super-observations utilized have been generated using an azimuthal averaging of 3.4° instead of 1.7°. This does not affect the interpretation of the results.

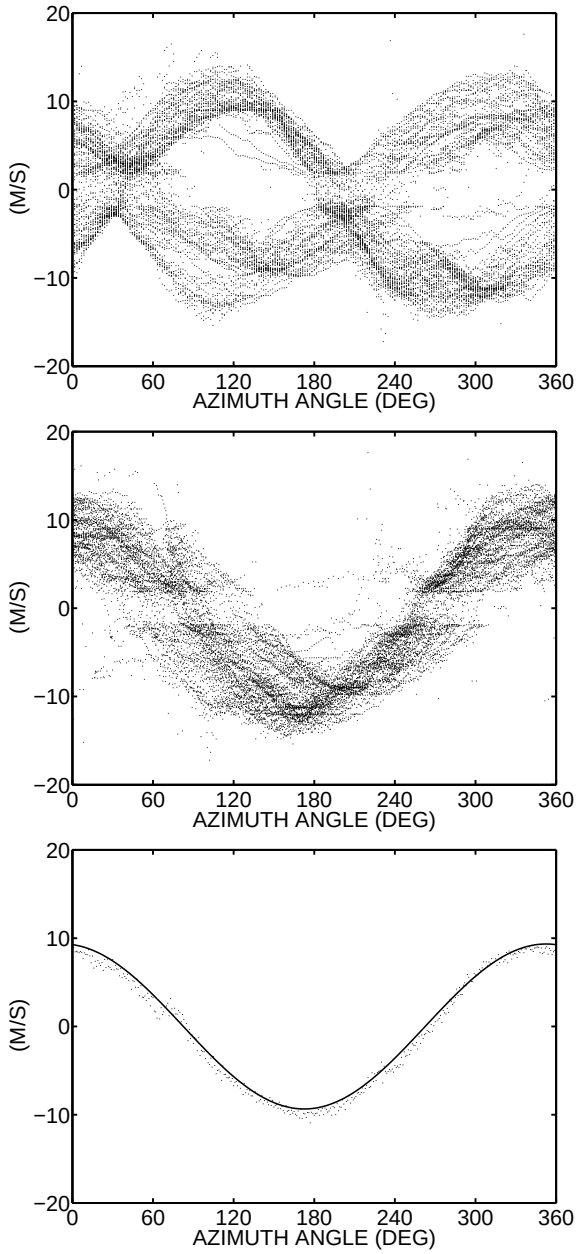

FIGURE 4.5. An illustration of the bias estimation method. Ca. 16 300 Doppler radar radial wind observations as a function of the azimuth angle (top panel). The Doppler radar radial wind observations after the rotation (middle panel). The bin-averaged observed radial wind speed (black dots) and the fitted cosine curve $v_r = 9.3m/s \cdot \cos(\delta - 7^\circ)$ (bottom panel). (Figure 2 of PAPER III)

study. A systematic feature in the HIRLAM model has been a slight over-prediction of mid-latitude depressions during recent years. The cyclogenesis of the depressions has been correctly predicted, but the low pressure systems have tended to remain too deep due to insufficient filling of the cyclones. Tijm (2003) suggested that the cyclone

decay forecast can be improved by modifying the formulation of the surface stress direction. Sass and Nielsen (2004) introduced a surface stress parameterization where the surface stress is turned clockwise (in the northern hemisphere) by a fixed amount. Consequently, the cross-isobar flow increases in the planetary boundary layer towards lower pressure. A validation study by Järvenoja (2004) indicates that the modified surface stress reduces the negative bias in surface pressure and the positive bias in the 10-metre winds, but upper air winds become slightly more biased.

Two one-month (January 2002) HIRLAM model experiments have been carried out to demonstrate the applicability of radar radial wind observations for NWP model validation. The two model experiments differ only in the surface stress parameterization feature described above. In the experiment designated as REF, the surface stress is parallel to the lowest model level wind, while in the experiment designated as ROT the surface stress has been rotated as suggested by Sass and Nielsen (2004). The model validation is done against three data sets: (i) radar radial wind observations from four radars in the Swedish radar network, (ii) conventional radiosonde wind observations from the HIRLAM model domain, and (iii) radiosonde wind observations from Sweden. The radar radial wind data set is five times larger than the radiosonde wind data set, and over 100 times larger than the subset of the Swedish radiosonde wind observations.

Figure 4.6 shows the vector wind bias for 6-hour forecasts as a function of height. In the top panel of Fig. 4.6 the bias is calculated against the radar wind observations. Near the ground and above 4 km altitude the vector wind bias is over 1 ms^{-1}. The vector wind bias takes into account both the wind speed and direction bias. In this case the bias is caused mainly by the wind direction bias below an altitude of 2 km. The 95% confidence intervals in the lowest 2 km are ± 0.03 ms^{-1}. Even though the bias is relatively large near the ground, it is evident that the bias is significantly larger for the experiment ROT than for the experiment REF.

The middle panel of Fig. 4.6 shows the vector wind bias for 6-hour forecasts calculated against radiosonde observations from the whole model domain. The magnitude of the bias is notably smaller for the radiosonde observations over the model domain than for the radar wind observations over Sweden. However, the result is consistent in that the bias is smaller for the REF experiment than for the ROT experiment. The 95% confidence intervals for the lowest 2 km (± 0.08 ms^{-1}) are almost three times as wide as the confidence intervals for the radar observations. The confidence intervals overlap at all altitudes, especially above an altitude of 1 km, and thus statistically significant conclusions about the differences between the experiments cannot be made.

The bottom panel of Fig. 4.6 shows the vector wind bias calculated against radiosonde observations from the Swedish radiosonde stations alone. The radiosonde vector wind bias is larger for Sweden than for the whole model domain. The 95% confidence intervals vary from ± 0.2 ms^{-1} to ± 0.4 ms^{-1}, and are largely overlapping. Again, no statistically significant conclusion can be drawn.

The validation study performed successfully shows that minor differences in NWP model versions can be distinguished and validated in a statistically confident manner

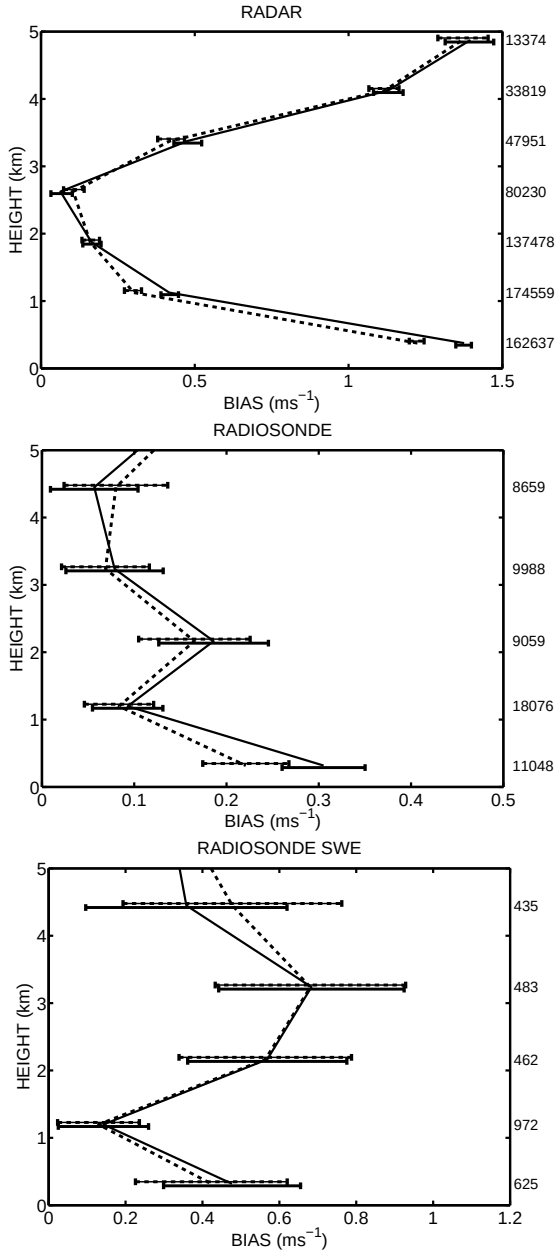

FIGURE 4.6. The vector wind bias as a function of height for radar wind observations (top panel). The solid line indicates the experiment with rotated surface stress and the dashed line indicates that without the rotation. Solid and dashed bars show the 95% confidence intervals. The number of observations is shown on the right side of the figure. The same is shown for radiosondes from the model integration area (middle panel) and for radiosondes from Sweden (bottom panel). (Figures 3 and 4 of PAPER IV)

by using radar radial wind observations. The results obtained are in good accordance with the earlier validation results presented by Järvenoja (2004). The large amount of

radar data results in narrow and non-overlapping confidence intervals, and allows one to make statistically significant conclusions about the differences between the model experiments.

5 CONCLUSIONS

The development of NWP modelling is focusing increasingly on high resolution and the forecasting of quickly-developing mesoscale phenomena. Doppler radars provide radial wind measurements with excellent spatial and temporal resolution. In this thesis, radar radial wind data assimilation tools have been developed, tested and exploited. Concluding remarks on the key questions raised in Chapter 1 are made in the following.

PAPER I introduces an observation operator for Doppler radar radial wind observations. The observation operator has been incorporated into the HIRLAM variational data assimilation system. The radar radial wind observation operator interpolates the vertical model wind profile to the observation location, and calculates the projection of the model wind vector on the radar pulse path. The refinements of the observation operator take into account the vertical broadening of the radar pulse volume, and the bending of the radar pulse path due to atmospheric conditions. The impact of the refinements on the observation minus model background (OmB) statistic have been studied. It can be concluded that modelling the broadening of the radar pulse volume improves the accuracy of the observation operator. The modelling of the radar pulse path bending has on average a neutral effect. However, also taking this aspect into account makes the observation operator more realistic, which can be very beneficial in some individual super- or subrefraction cases.

The advantage of variational data assimilation is that the exploitation of indirect observations of the model variables is straightforward, and unknown errors introduced by preprocessing of the observations are avoided. In the case of Doppler radar radial wind observations, a certain amount of preprocessing is, however, found to be beneficial, as discussed in PAPER II. Radar radial wind observations are modelled within observation errors which consist of instrumental, modelling, and representativeness errors. The impact of the random part of the instrumental and representativeness errors can be decreased by calculating spatial averages, so called super-observations, from the raw observations. HIRLAM model experiments indicate that the super-observation generation clearly improves the fit of the radial wind observations to the model in terms of OmB standard deviation. However, averaging of observations over a wide azimuthal angle degrades the quality of the super-observation and should be avoided.

Monitoring the quality of the observations is an important aspect, especially when a new observation type is introduced into a data assimilation system. In PAPER III it is demonstrated that for Doppler radar radial wind observations, the conventional way to calculate OmB bias does not provide correct information about systematic differences in the observed and modelled wind speeds and directions. In fact, aggregating the OmB values over different azimuth directions in the bias calculation can result in a zero bias even in the presence of significant systematic differences. This is due to the azimuthal symmetry of the radial wind component. The bias estimation method introduced in PAPER III resolves the problem by utilising the knowledge of NWP model

wind direction at the observation location. A reference direction is chosen and a rotation angle is defined as a difference between the reference wind direction and the model wind direction. The azimuth angle corresponding to the observation is rotated by adding the rotation angle to it. By calculating azimuth bin average for the rotated observations and for their model counterparts, and by fitting the radial wind equation to the bin averages, reliable estimates of the wind speed and wind direction bias can be provided. Random errors, on the other hand, can be expected to be evenly distributed over all azimuth directions. Thus, there is no information loss when the radial wind OmB standard deviation is studied directly.

The observation operator developed, together with the bias estimation method, also enables the exploitation of the Doppler radar radial wind observations for NWP model validation. The one-month model experiments performed in PAPER IV with HIRLAM model versions differing only in a surface stress parameterization detail indicate that the use of radar wind observations in NWP model validation is very beneficial. The large amount of radar observations results in narrow and non-overlapping confidence intervals, unlike the validation against radiosonde wind observations in the case studied. This allows one to make statistically significant conclusions about the differences between the model experiments.

An interesting and important question not covered in this thesis is the impact of using Doppler radar radial wind observations on the NWP model analysis and forecasts. This is the subject of ongoing research in the HIRLAM framework, and the tools developed in this thesis are utilised in the work. The results will be published in peer-reviewed journals in the future.

REFERENCES

Alberoni, P P, Ducrocq, V, Gregoric, G, Haase, G, Holleman, I, Lindskog, M, Macpherson, B, Nuret, M and A Rossa, 2001: Cost Action 717 – Quality and Assimilation of Radar Data – A review. 55 pp.

Albers, S, 1995: The LAPS Wind Analysis. *Weather and Forecasting*, **10**, 342–352.

Berger, H, Forsythe, M, Eyre, J and S Healy, 2004: A superobbing scheme for atmospheric motion vectors. *Proceedings of The seventh international winds workshop*, **EUM P.42**, 119–126.

Bouttier, F and G Kelly, 2001: Observing-system experiments in the ECMWF 4D-Var data assimilation system. *Q. J. R. Meteorol. Soc*, **127**, 1469–1488.

Caumont, O, Wattrelot, É, Ducrocq, V, Jaubert, G and F Bouttier, 2006a: First results of 1D+3DVAR assimilation of radar reflectivities. *Proceedings of the Fourth European Conference on Radar Meteorology and Hydrology*, 539–542.

Caumont, O, Ducrocq, V, Delrieu, G, Gosset, M, Pinty, J P, Parent Du Châtelet, J, Andrieu, H, Lemaître, Y and G Scialom, 2006b: A radar simulator for high-resolution nonhydrostatic models. *J. Atmos. Oceanic Tech.*, **23**, 1049–1066.

Charney, J and A Eliassen 1949: A numerical method for predicting the perturbations of the midlatitude westerlies. *Tellus*, **1**, 38–54.

Charney. J, Fjørtoft, R and J von Neuman, 1950: Numerical integration of the barotropic vorticity equation. *Tellus*, **2**, 237–254.

Courtier, P and O Talagrand, 1990: Variational data assimilation of meteorological observations with the direct and adjoint shallow water equations. *Tellus*, **42A**, 531–549.

Courtier, P, Thépaut, J N and A Hollingsworth, 1994: A strategy for operational implementation of 4D-Var, using an incremental approach. *Q. J. R. Meteorol. Soc.*, **120**, 1367–1387.

Daley, R, 1991: *Atmospheric Data Analysis*. Cambridge University Press, 457 pp.

Dazhang, T, Geotis, S G, Passarelli Jr, R E, Hansen, A L and C L Frush, 1984: Evaluation of an alternating-PRF method for extending the range of unambiguous Doppler velocity. Preprints, 22nd Conf. on Radar Meteorology, Zurich, Switzerland, Amer. Meteor. Soc., 523–527.

Doviak, R J and D S Zrnić, 1993: *Doppler radar and weather observations*. Second edition. San Diego Academic Press, Inc., 562 pp.

Eresmaa, R and H Järvinen, 2006: An observation operator for ground-based GPS slant delays. *Tellus*, **58A**, 131–140.

Eresmaa, R, Healy, S, Järvinen, H and K Salonen, 2008: Implementation of a ray-tracing operator for ground-based GPS Slant Delay observation modeling. *J. Geophys. Res.*, **113**, D11114, doi:10.1029/2007JD009256.

Eyre, J R, 1990: Progress on direct use of satellite sounding radiances in numerical weather prediction. Preprints WMO International Symposium on Assimilation of Observations in Meteorology and Oceanography; Clermont- Ferrand, France; 9-13 July 1990; WMO Report, pp. 117–121.

Evensen, G, 1994: Sequential data assimilation with a nonlinear quasi-geostrophic model using Monte Carlo methods to forecast error statistics. *J. Geophys. Res.*, **99**, 10143–10162.

Gabella, M and R Notarpietro, 2002: Ground clutter characterization and elimination in mountainous terrain. *ERAD Publication Series*, Vol. 1, 312–317.

Gandin, L S, 1963: Objective analysis of meteorological fields, *Gidrometeorologich-eskoe Izdatelstvo*, Leningrad. English translation by Israeli Program for Scientific Translations, Jerusalem, 1965.

Gustafsson, N, Berre, L, Hörnquist, S, Huang, X-Y, Lindskog, M, Navascués, B, Mogensen, K S and S Thorsteinsson, 2001: Three-dimensional variational data assimilation for a limited area model. Part I: General formulation and the background error constraint. *Tellus*, **53A**, 425–446.

Haase, G and T Landelius, 2004: Dealiasing of Doppler radar velocities using a torus mapping. *J. Atmos. and Oceanic Tech.*, **21**, 1566–1573.

Hart, T, Bourke, W, Steinle, P and R Seaman, 1993: Impact of higher-resolution satellite soundings of temperature and moisture on large-scale numerical weather prediction. *Mon. Wea. Rev.* **121**, 1746–1758.

Holton, J, 1992: *An introduction to dynamic meteorology*. 3rd edition. Academic Press, San Diego. 511 pp.

Houtekamer, P L and H L Mitchell, 1998: Data assimilation using an ensemble Kalman filter technique. *Mon. Wea. Rev.*, **126**, 796–811.

Järvenoja S, 2004: Experimentation with a modified surface stress. *HIRLAM Newsletter*, **45**, 113–123. Available online at
http://hirlam.org/open/publications/NewsLetters.

Kalman, R E, 1960: A new approach to linear filtering and prediction problems. *Journal of Basic Engineering*, **82**, 35–45.

Kalnay, E, Jusem, J C and J Pfaendtner, 1985: The relative importance of mass and wind data in the FGGE observing system. Proceedings of the NASA Symposium on Global Wind Measurements, 1–5.

Kalnay, E, 2003: *Atmospheric modeling, data assimilation and predictability*. Cambridge University Press, United Kingdom, 341 pp.

Lange, A A, 2001: Simultaneous Statistical Calibration of the GPS signal delay measurements with related meteorological data. *Phys. Chem. Earth (A)*, **26**, 471–473.

Larkin, R P, 1991: Sensitivity of NEXRAD algorithms to echoes from birds and insects. *Prepr., Radar Meteorol. Conf., 25th*, 203–205.

Lewis, J and J Derber, 1985: The use of adjoint techniques to solve variational adjustment problem with advective constraint. *Tellus*, **37A**, 309–322.

Lindskog, M, Järvinen, H and D B Michelson, 2000: Assimilation of Radar Radial Winds in the HIRLAM 3D-Var. *Phys. Chem. Earth (B)*, **25**, 1243-1249.

Lindskog, M, Gustafsson, N, Navascués, B, Mogensen, K S, Huang, X-Y, Yang, X, Andræ, U, Berre, L, Thorsteinsson, S and J Rantakokko, 2001: Three-dimensional variational data assimilation for a limited area model. Part II: Observation handling and assimilation experiments. *Tellus*, **53A**, 447–468.

Lindskog, M, Salonen, K, Järvinen, H and D B Michelson, 2004: Doppler radar wind data assimilation with HIRLAM 3DVAR. *Mon. Wea. Rev.*, **132**, 1081–1092.

Lorenc, A C, 1981: A global three dimensional multivariate statistical interpolation scheme. *Mon. Wea. Rev.*, **109**, 701–721.

Lorenc, A C, 1986: Analysis methods for numerical weather prediction. *Q. J. R. Meteorol. Soc.*, **112**, 1177–1194.

Lorenz, E N, 1965: A study of the predictability of a 28-variable atmospheric model. *Tellus*, **17**, 321–333.

Lynch, P, 2006: *The Emergence of Numerical Weather Prediction: Richardson's Dream*. Cambridge University Press. 279 pp.

Lönnberg, P and D Shaw, 1983: Research manual 1. ECMWF data assimilation. Scientific documentation. 103 pp.

Michelson, D, Einfalt, T, Holleman, I, Gjertsen, U, Friedrich, K, Haase, G, Lindskog, M and A Jurczyk, 2004: Weather radar data quality in europe: Quality control and characterization. COST 717 Working document. Available online at http://www.smhi.se/cost717/.

Montmerle, T and C Faccani 2008: Mesoscale assimilation of radial velocities from Doppler radar in pre-operational framework. *Mon. Wea. Rev.*, in press.

Niemelä, S and C Fortelius, 2005: Applicability of large-scale convection and condensation parameterization to meso-γ-scale HIRLAM: A case study of a convective event. *Mon. Wea. Rev.*, **133**, 2422–2435.

Ohring, G, Lord, S, Derber, J, Mitchell, K and M Ji, 2002: Applications of satellite remote sensing in numerical weather and climate prediction. *Advances in Space Research*, **30**, 2433–2439.

Palmer T N, 1993: Extended-range atmospheric prediction and the Lorenz model. *Bull. Amer. Met. Soc*, **74**, 49–65.

Peura, M, 2002: Computer vision methods for anomaly removal. *ERAD Publication Series*, Vol. 1, 312–317.

Pielke, R A, 2002: *Mesoscale meteorological modeling*. 2nd edition. Academic Press. San Diego. 676 pp.

Pirttilä, J, Lehtinen, M S, Huuskonen, A and M Markkanen, 2005: A Proposed Solution to the Range-Doppler Dilemma of Weather Radar Measurements by Using the SMPRF Codes, Practical Results, and a Comparison with Operational Measurements. *J. Applied Met.*, **44**, 1375–1390.

Probert-Jones, J R, 1962: The radar equation in meteorology. *Q. J. R. Meteor. Soc.*, **88**, 485–495.

Ray, P and C Ziegler, 1977: De-aliasing first moment Doppler estimates. *J. Appl. Meteor.*, **16**, 563–564.

Richardson, L F, 1922: *Weather Prediction by Numerical Process*. Cambridge University Press. 236 pp.

Rikus L, 1997: Application of a scheme for validating clouds in an operational global NWP model. *Mon. Wea. Rev.*, **125**, 1615–1636.

Rossby, C G, 1938: On the mutual adjustment of pressure and velocity distributions in certain simple current systems, II. *J. of Marine Research*, **1**, 239–263.

Sass B H and N W Nielsen, 2004: Modelling of the HIRLAM surface stress direction. *HIRLAM Newsletter*, **45**, 105–112. Available online at http://hirlam.org/open/publications/NewsLetters.

Sauvageot, H, 1992: *Radar Meteorology*. Artech house, Inc., Norwood, USA, 366 pp.

Seko, H, Kawabata, T, Tsuyuki, T, Nakamura, H and K Koizumi, 2004: Impacts of GPS-derived Water Vapor and Radial Wind Measured by Doppler Radar on Numerical Prediction of Precipitation. *J. Met. Soc. Japan*, **82**, 473–489.

Shuman, F, 1989: History of numerical weather prediction at the National Meteorological Center. *Weather and forecasting*, **4**, 286–296.

Sirmans D, Zrnić, D and B Bumgarner, 1976: Extension of maximum unambiguous Doppler velocity by use of two sampling rates. Preprints, 17th Conf. on Radar Meteorology, Seattle, WA, Amer. Meteor. Soc., 23–28.

Sun, J and N A Crook, 1997: Dynamical and microphysical retrieval from Doppler radar observations using a cloud model and its adjoint. Part I: Model development and simulated data experiments. *J. Atmos. Sci.*, **54**, 1642–1661.

Swarbrick, S, 2006: Assimilation of Doppler radar radial winds. Proceedings of ERAD 2006, 527–530.

Talagrand, O, 1997: Assimilation of observations, an introduction. *J. Met. Soc. Japan*, Special issue **75**, 1B, 191–209.

Thompson P D, 1957: Uncertainty of initial state as a factor in the predictability of large-scale atmospheric flow patterns. *Tellus*, **9**, 275–295.

Tijm S, 2003: Different aspects of CPR/CLJ. *HIRLAM Newsletter*, **44**, 49–60. Available online at
http://hirlam.org/open/publications/NewsLetters.

Undén, P, Rontu, L, Järvinen, H, Lynch, P, Calvo, J, Cats, G, Cuxart, J, Eerola, K, Fortelius, C, Garcia-Moya, J A, Jones, C, Lenderlink, G, McDonald, A, McGrath, R, Navascues, B, Nielsen, NW, Ødegaard, V, Rodriguez, E, Rummukainen, M, Rõõm, R, Sattler, K, Hansen, B S, Savijärvi, H, Schreur, B W, Sigg, R, The, H and A Tijm, 2002: HIRLAM-5 Scientific Documentation. HIRLAM-5 Project, c/o Per Undén SMHI, SE-601 76 Norrköping, Sweden. Available online at
http://hirlam.org/open/publications/SciDoc_Dec2002.pdf

Untch, A, Miller, M, Hortal, M, Buizza, R and P Janssen, 2006: Towards a global meso-scale model: The high-resolution system T799L91 and T399L62 EPS. *ECMWF Newsletter No. 108*, 6–13.

Xiao, Q, Sun, J, Lee, W, Lim, E, Guo, Y, Barker, D and Y-H Kuo, 2003: Assimilation of Doppler radar observations with a regional 3D-Var system: a heavy rainfall case study. Proceedings of the 31st AMS International Conference on Radar Meteorology, 165–168.

Xiao, Q, Kuo, Y-H, Sun, J, Lee, W-C, Lim, E, Guo, Y-R and D Barker, 2005: Assimilation of doppler radar opbservations with a regional 3DVAR system: Impact of Doppler velocities on forecasts of a heavy rainfall case. *J. Appl. Meteor.*, **44**, 768–788.

Vedel, H and X-Y Huang, 2004: Impact of ground based GPS data on numerical weather prediction. *J. Meteor. Soc. Japan*, **82**, 459–472.

Veerlan, M and A W Heemink, 1997: Tidal flow forecasting using reduced rank square root filters. *Stoch. Hydrology and Hydraulics*, **11**, 349–368.